Journal of Power Sources 245 (2014) 637–643

Contents lists available at SciVerse ScienceDirect

Journal of Power Sources

journal homepage: www.elsevier.com/locate/jpowsour

Effect of multiwalled carbon nanotubes with different specific surface areas on the stability of supported Pt catalysts

Lei Zhao, Zhen-Bo Wang*, Xu-Lei Sui, Ge-Ping Yin

School of Chemical Engineering and Technology, Harbin Institute of Technology, No. 92 West-Da Zhi Street, Harbin 150001, China

HIGHLIGHTS

- Effect of MCNTs with various specific surface areas on stability of Pt catalysts is investigated.
- Pt/MCNTs-250 catalysts show the highest initial ESA and the activity for methanol electrooxidation.
- Electrochemical activity of the catalysts reduces with the decrease of the surface areas of MCNTs.
- Considering the activity and stability, the optimized specific surface area of MCNTs is 120 $m^2\ g^{-1}$.

GRAPHICAL ABSTRACT

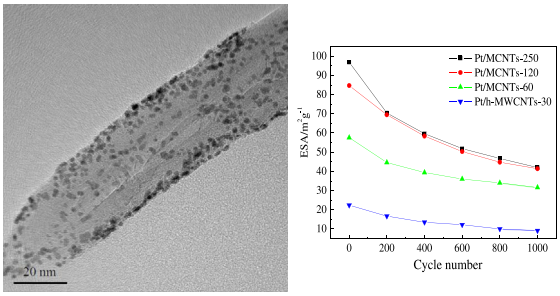

ARTICLE INFO

Article history:
Received 30 May 2013
Received in revised form
3 July 2013
Accepted 3 July 2013
Available online 13 July 2013

Keywords:
Proton exchange membrane fuel cell
Carbon nanotubes
Specific surface area
Platinum catalyst
Stability

ABSTRACT

Pt/MCNTs catalysts have been synthesized by the microwave-assisted polyol process (MAPP). Effect of multiwalled carbon nanotubes (MCNTs) with different specific surface areas on the stability of supported Pt catalysts has been investigated. The obtained Pt/MCNTs catalysts are characterized by X-ray diffraction (XRD), Energy dispersive analysis of X-ray (EDAX), transmission electron microscopy (TEM), cyclic voltammograms (CV), electrochemical impedance spectroscopy (EIS), and accelerated potential cycling tests (APCT) to present the stability of the catalysts. The experimental results indicate that the original electrochemically active specific surface areas (ESA) and the activity for methanol electrooxidation of the catalysts decrease with the decreasing of the specific surface areas of MCNTs, and the Pt/MCNTs-250 (MCNTs with pristine specific surface of 250 $m^2\ g^{-1}$, below the same) catalysts show the best initial electrochemical activity. However, the activity of the Pt/MCNTs-250 is very close to that of the Pt/MCNTs-120 and the stability of the Pt/MCNTs-60 catalyst is the best after 1000 cycles APCT. Considering the factors of the activity and stability comprehensively, the optimized specific surface area of MCNTs in the Pt/MCNTs catalysts is 120 $m^2\ g^{-1}$.

1. Introduction

Proton exchange membrane fuel cell (PEMFC) is a low-temperature fuel cell (typically less than 100 °C) with a polymer electrolyte membrane. PEMFC has received worldwide attention because of its high energy density, low temperature operation, fast start-up, and the potential application in automotive and portable electronics [1–4]. The PEMFC is considered to be promising power source that is appropriate for stationary and mobile applications [5,6].

The commercial application of the fuel cells is expected to lead to further improvements in performance, durability, and cost [7,8]. Carbon black [9–11] is still the most widely used catalyst support for its high surface area, good electronic conductivity, and appropriate pore structure. However, the corrosion of carbon black in the catalysts is still the biggest obstacle to its commercialization.

* Corresponding author. Tel.: +86 451 86417853; fax: +86 451 86418616.
E-mail address: wangzhenbo1008@yahoo.com.cn (Z.-B. Wang).

0378-7753/$ – see front matter © 2013 Elsevier B.V. All rights reserved.
http://dx.doi.org/10.1016/j.jpowsour.2013.07.027

Novel carbon materials such as carbon nanotubes [12], carbon nanofibers [13], carbon nanocages [14], carbon nanohorns [15] and graphene [16] etc. have been extensively studied as catalyst supports for PEMFCs. Carbon nanotubes (CNTs) are considered to be a more attractive candidate owing to the nanometer size, high specific surface area, nice corrosion resistance, special electronic and mechanical properties [17–19]. Matsumoto et al. [20] reported a Pt-deposited carbon nanotube (CNT) shows higher performance than a commercial Pt-deposited carbon black (CB) with reducing 60% Pt loading per electrode area in polymer electrolyte fuel cells (PEFCs) below 500 mA cm^{-2}. For carbon nanotube supported catalysts, it is found that the effective attachment of Pt nanoparticles uniformly dispersed onto CNTs remains a challenge. An improved method is to functionalize the external walls of nanotubes through oxidation. The pretreatment is probably the most common way of surface activation since a mixture of strong acids will typically not only remove the impurities on the surface of CNTs but also introduce the functional groups that are conducive to the deposition of the Pt metal ions.

The previous reports have shown that CNTs are more corrosion resistant than carbon black used as a catalyst support [21]. However, so far, the effect of MCNTs with different specific surface areas on the stability of Pt-based catalysts prepared by the microwave-assisted polyol process (MAPP) has not been studied yet. In this paper, multiwalled carbon nanotubes (MCNTs) have been treated with a mixture of concentrated H_2SO_4 and 70% HNO_3 (8 mol L^{-1} H_2SO_4 + 8 mol L^{-1} HNO_3). Pt/MCNTs catalysts have been synthesized by the microwave-assisted polyol process (MAPP). X-ray diffraction (XRD), Energy dispersive analysis of X-ray (EDAX), transmission electron microscopy (TEM), cyclic voltammograms (CV), electrochemical impedance spectroscopy (EIS) and accelerated potential cycling tests (APCT) have been applied to examine the effect of different specific surface areas of MCNTs on performance of Pt/MCNTs catalysts.

2. Experimental

2.1. Materials

Hexachloroplatinic acid ($H_2PtCl_6 \cdot 6H_2O$) was purchased from Shanghai, China. 5 wt% Nafion solution was purchased from Dupont. Multiwalled carbon nanotubes (MCNTs) with pristine specific surface areas of 60, 120, 250 m^2 g^{-1} and helical multiwalled carbon nanotubes (h-MWCNTs) with pristine specific surface area of 30 m^2 g^{-1} were obtained from Chengdu Institute of Organic Chemistry, China. Except where specified, all chemicals were of analytical grade and used as received.

2.2. Pretreatment of MCNTs

Functionalized MCNTs and h-MWCNTs were prepared using a conventional mixed acid treatment method. The raw MCNTs were dispersed in a mixture of concentrated H_2SO_4 and 70% HNO_3 (8 mol L^{-1} H_2SO_4 + 8 mol L^{-1} HNO_3) and sonicated for 5 h. Then the resulting functionalized MCNTs were washed repeatedly with ultrapure water (18.2 MΩ cm) until the pH value was close to 7. The functionalized MCNTs powder was dried in a vacuum oven at 85 °C for 10 h.

2.3. Catalyst preparation

Pt/MCNTs catalysts with the Pt metal loading of 20 wt% were synthesized by a microwave-assisted polyol process (MAPP). Briefly, 40 mg functionalized MCNTs were dispersed in 25 mL ethylene glycol (EG) solvent under ultrasonic treatment (from Shanghai, 53 kHz, 280 W) for 1 h. Then H_2PtCl_6–EG solution was added into the uniform ink with agitation for 3 h. The pH value of the ink was then adjusted to 12.0 and the suspension was subjected to consecutive microwave heating for 64 s. After cooling to room temperature, the pH value of the solution was adjusted to about 3. The mixture was kept stirring for 12 h and then the product was washed repeatedly with ultrapure water (18.2 MΩ cm) until no Cl^- ions were detected (The filtrate was titrated with $AgNO_3$ solution, until there was no white precipitate). The homemade Pt/MCNTs catalysts were dried for 5 h at 80 °C in a vacuum oven and then stored in a vacuum vessel.

2.4. Physical characterization

Brunauer–Emmett–Teller (BET) specific surface area of the functional MCNTs was examined via nitrogen adsorption experiments at 77 K using a QUADRASORB SI analyzer. X-ray photoelectron spectroscopy (XPS) analysis was carried out to determine the surface properties of the MCNTs with a physical electronics PHI model 5700 instrument. The Al X-ray source was operated at 250 W and the take-off angle of the sample to analyzer was 45°. Survey spectra were collected at pass energy (PE) of 187.85 eV over a binding energy range from 0 eV to 1300 eV. High binding energy resolution multiplex data for the individual elements were collected at a PE of 29.55 eV. During all XPS experiments, the pressure inside the vacuum system was maintained at 1×10^{-9} Pa. Before the analysis above, all the samples were dried under vacuum at 80 °C overnight. X-ray diffraction (XRD) analysis of as-prepared catalysts was carried out with the D/max-RB diffractometer (made in Japan) using a Cu Kα X-ray source operating at 45 kV and 100 mA, scanning at a rate of 4° min^{-1} with an angular resolution of 0.05° of the 2θ scan to get the XRD pattern. Hitachi-S-4700 analyzer was coupled to a scanning electron microscope (SEM, Hitachi Ltd. S-4700) for a rapid Energy dispersive analysis of X-ray (EDAX) of chemical composition. The samples were supported on the aluminum foil to eliminate the influence of the conductive carbon tape. The sample surface was impinged from the normal angle for 100 s by the X-ray incident electron beam with energies ranging from 3 to 30 keV. Transmission electron microscopy (TEM) for the catalyst samples were taken by a TECNAI G2 F30 field emission transmission electron microscope. Before taking the electron micrographs, the samples were finely ground and ultrasonically dispersed in alcohol, and a drop of the resultant dispersion was deposited and dried on a standard copper grid coated with carbon film. The applied voltage was 300 kV.

2.5. Electrochemical measurements

All electrochemical measurements were carried out in a standard three-electrode cell using a CHI 650E electrochemical analysis instrument at an ambient temperature. Working electrodes were prepared as follows: 2.0 mg catalyst in 2.0 mL mixture of ethanol and ultrapure water (V/V = 1:1) was ultrasonicated for 20 min. Then, 10 μL of this ink was transferred onto a glassy carbon disk (GC, 4 mm diameter), and onto which 5 μL of a dilute aqueous Nafion® solution (5 wt% solution in a mixture of lower aliphatic alcohols and ultrapure water) was added. A platinum wire was used as the counter electrode and the Hg/Hg_2SO_4 (−0.68 V relative to reversible hydrogen electrode, RHE) was used as the reference electrode. The cyclic voltammograms (CV) were recorded within a potential range from 0.05 V to 1.2 V (vs. RHE). EIS were usually obtained at frequencies between 0.01 Hz and 100 kHz with 12 points per decade. The amplitude of the sinusoidal potential signal was 5 mV.

To investigate the stability of catalysts, the accelerated potential cycling test (APCT) within the potential range of 0.6–1.2 V (vs. RHE)

was applied. The electrochemical active specific surface areas (ESA) [22] of platinum with coulombic charges accumulated during hydrogen adsorption or desorption after correcting for the double-layer charging current from the CVs can be calculated [23]:

$$\mathrm{ESA} = \frac{Q_{\mathrm{H}}}{0.21 \times M_{\mathrm{Pt}}} \quad (1)$$

where Q_{H} (mC) is the charge due to the hydrogen adsorption/desorption in the hydrogen region of the CVs, 0.21 mC cm^{-2} is the electrical charge associated with monolayer adsorption of hydrogen on Pt, and M_{Pt} is the loading of Pt metal on the working electrode.

3. Results and discussion

3.1. Physical characteristics of homemade various Pt/MCNTs catalysts

The BET specific surface areas of the functional MCNTs are 152.2 $m^2\ g^{-1}$, 65.2 $m^2\ g^{-1}$, 49.5 $m^2\ g^{-1}$, 23.3 $m^2\ g^{-1}$ compared with the pristine specific surface area of 250 $m^2\ g^{-1}$, 120 $m^2\ g^{-1}$, 60 $m^2\ g^{-1}$, 30 $m^2\ g^{-1}$, respectively. It can be observed that the specific surface area decreases significantly after the functionalization. The reason may be that the impurities and ash contained in MCNTs are removed, and some short MCNTs are dissolved during the treatment of the mixed acid.

XPS analyses are applied to examine the surface states of these MCNTs before and after the functionalization. Fig. 1 shows the C1s regions of the XPS spectra of the pristine and functionalized MCNTs. The binding energies of each component along with their relative intensities are provided in Table 1. It is found that amount of surface functional groups with oxygen contents, such as carboxyl (—COOH), hydroxyl (—OH) increase after the functionalization. It can be also seen the ratio of sp^3 hybridization carbon of functionalized MCNTs is higher than the pristine MCNTs, indicating that the functional groups have been introduced to the MCNTs. As a result, the functionalized MCNTs are suitable for anchoring Pt metal ions.

The XRD patterns of Pt/MCNTs catalysts with various specific surface areas of MCNTs are shown in Fig. 2. The pattern represents the characteristic peaks of a crystalline face-centered-cubic (fcc) Pt phase as it shows the planes (111), (200), (220), and (311) at the corresponding diffraction positions. The diffraction peak observed at 23–26° can be attributed to the hexagonal graphite structure (002), which shows that MCNTs have good electric conductivity [24]. For purposes of simplicity and convenience, Pt/MCNTs catalysts with MCNTs pristine specific surface areas of 250 $m^2\ g^{-1}$, 120 $m^2\ g^{-1}$, 60 $m^2\ g^{-1}$, and h-MWCNT of 30 $m^2\ g^{-1}$ are denoted as Pt/MCNTs-250, Pt/MCNTs-120, Pt/MCNTs-60 and Pt/h-MWCNTs-30, respectively. The amount of Pt deposited on the MCNTs is checked by Energy dispersive analysis of X-ray (EDAX). The Pt contents are 18.35 wt%, 18.72 wt%, 18.80 wt% and 17.12 wt% in Pt/MCNTs-250, Pt/MCNTs-120, Pt/MCNTs-60 and Pt/h-MWCNTs-30, respectively, which are close to the theoretical values of 20 wt%.

TEM images with associated size distributions of Pt/MCNTs-250, Pt/MCNTs-120, Pt/MCNTs-60 and Pt/h-MWCNTs-30 are shown in Fig. 3. It can be observed that fine Pt nanoparticles disperse uniformly on the MCNTs. Pt nanoparticle sizes slightly

Table 1
Results of the fits of the C1s spectra.

Samples	Species	Bond	Binding energy/eV	Peak half width/eV^{-1}	Relative content/%
Pristine MCNTs	C 1s	sp^2-C	284.45	1.61	86.94
		sp^3-C	285.22	2.00	4.50
		C—OR	286.21	1.27	6.96
		C═O	287.31	1.26	1.07
		COOR	289.01	1.38	0.54
Functionalized MCNTs	C 1s	sp^2-C	284.43	1.55	79.20
		sp^3-C	285.20	2.89	6.07
		C—OR	286.18	1.66	10.35
		C═O	287.57	2.04	1.29
		COOR	288.50	2.45	2.39
		Anti π bond	291.18	1.66	0.70

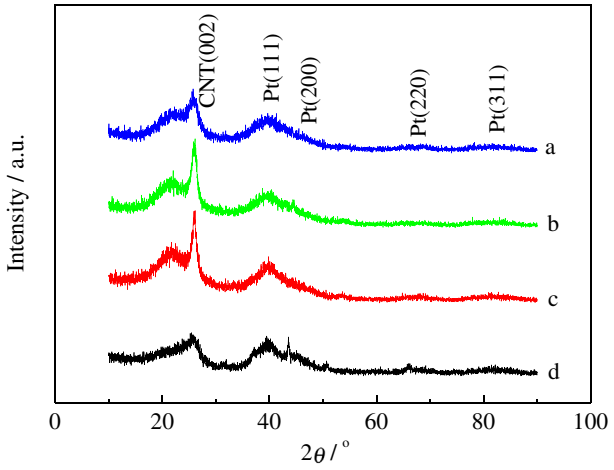

Fig. 2. XRD patterns of Pt/MCNTs catalysts with various specific surface areas of MCNTs: (a) 250 $m^2\ g^{-1}$, (b) 120 $m^2\ g^{-1}$ (c) 60 $m^2\ g^{-1}$, and (d) h-MWCNTs with specific surface area 30 $m^2\ g^{-1}$.

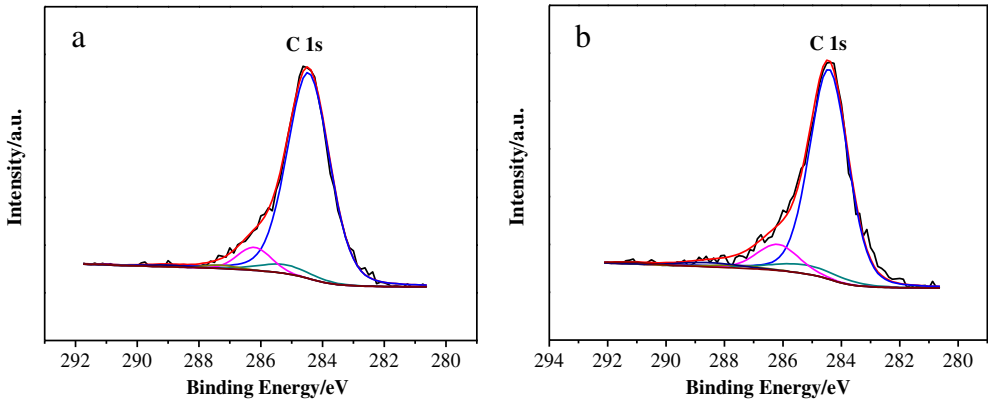

Fig. 1. The C1s regions of the XPS spectrum of the pristine (a) and functionalized (b) MCNTs.

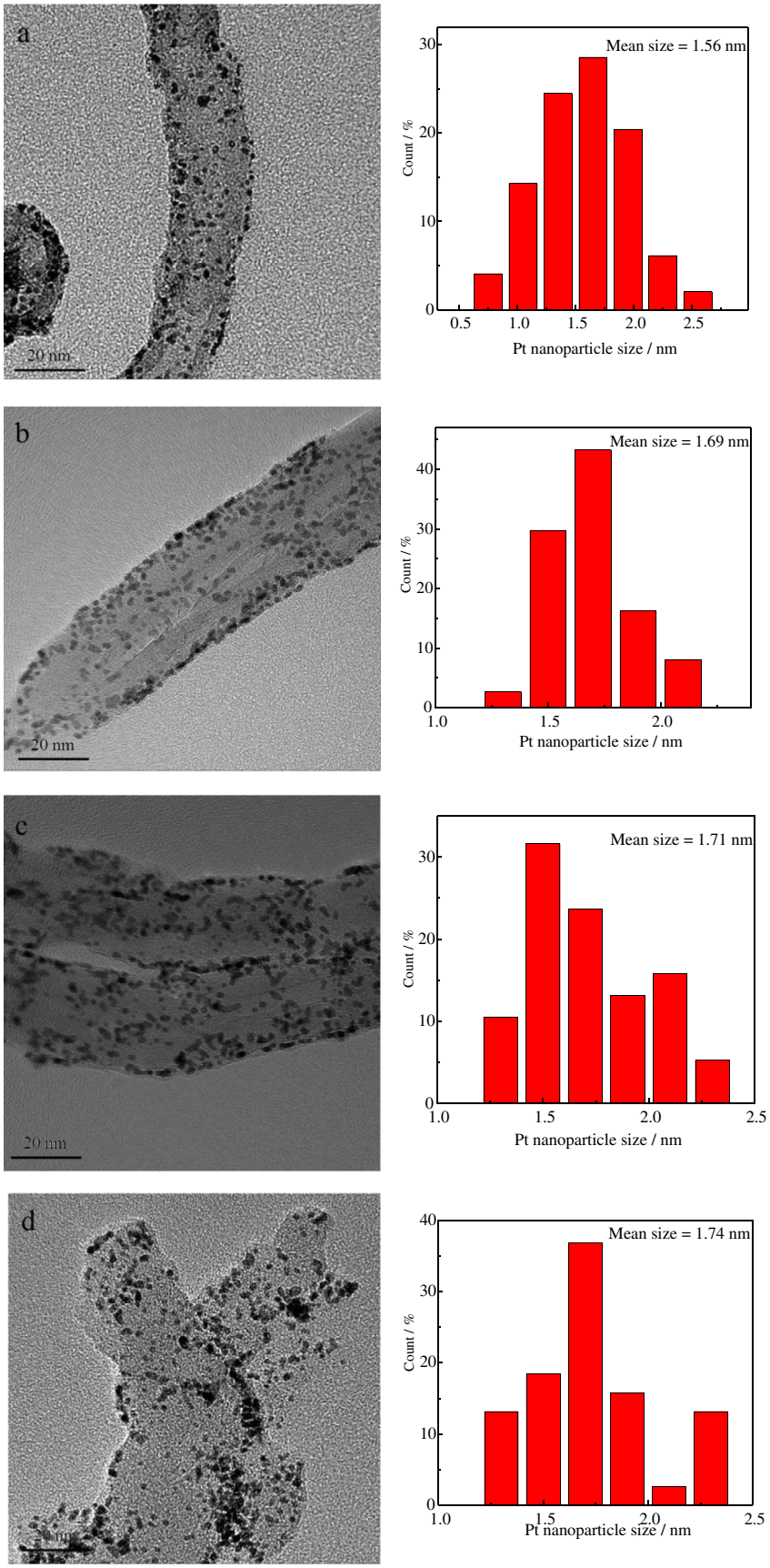

Fig. 3. TEM images and the size distributions of Pt/MCNTs catalysts with various specific surface areas of MCNTs: (a) 250 $m^2\ g^{-1}$, (b) 120 $m^2\ g^{-1}$, (c) 60 $m^2\ g^{-1}$, and (d) h-MWCNTs with specific surface area 30 $m^2\ g^{-1}$.

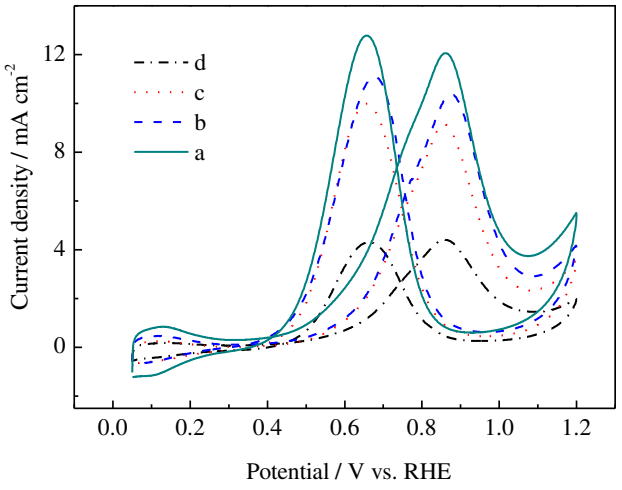

Fig. 4. Cyclic voltammograms in 0.5 mol L^{-1} CH_3OH and 0.5 mol L^{-1} H_2SO_4 for Pt/MCNTs with various specific surface areas of MCNTs: (a) 250 m^2 g^{-1}, (b) 120 m^2 g^{-1}, (c) 60 m^2 g^{-1}, and (d) h-MWCNTs with specific surface area 30 m^2 g^{-1}. Scanning rate: 50 mV s^{-1}; test temperature: 25 °C.

increase with the decreasing of specific surface areas of MCNTs. The mean size of Pt nanoparticles on Pt/MCNTs-250 is estimated to be 1.56 nm which is the smallest with narrow particle size distribution, whereas some aggregation and growth of Pt particles on Pt/h-MWCNTs-30 catalysts can be seen. It is well known that the distribution and a smaller particle size of Pt nanoparticles on the supports are key factors for enhancing its electrocatalytic activity and efficiency [25,26]. In our previous work, we [27] reported a Pt-deposited multiwalled carbon nanotubes (MCNTs) which were not functionalized, were synthesized in the same way. It can be found that Pt nanoparticles deposited into a sheet with agglomerate on the pristine MCNTs, while more uniformly on the functionalized MCNTs in present work. The results indicate that the activity of Pt/MCNTs catalysts decreases with the decreasing of specific surface areas of MCNTs.

3.2. Electrochemical characteristics of homemade various Pt/MCNTs catalysts

Fig. 4 shows the CV curves of Pt/MCNTs with various specific surface areas of MCNTs for methanol electrooxidation in a solution of 0.5 mol L^{-1} H_2SO_4 containing 0.5 mol L^{-1} CH_3OH at 25 °C. It can be seen that the onset potential and peak potential of Pt/MCNTs with various specific surface areas of MCNTs for methanol electrooxidation are almost the same, about 0.60 V and 0.86 V (vs. RHE), respectively. However, significant differences in peak current density are observed, the current measured on Pt/MCNTs-250 reaches 12.0 mA cm^{-2}, which exhibits the highest current density at all corresponding samples. Comparison of the CV curves of all corresponding samples reveals that the peak current density decreases with the decreasing of the specific surface areas of MCNTs. The results above indicate that the Pt/MCNTs-250 shows better catalytic performance for methanol electrooxidation than other samples. It is because that it has the smallest particle size which is in accordance with the TEM results above and narrow size dispersion on MCNTs-250 support.

Electrochemical impedance spectroscopy (EIS) is an effective measurement to determine the charge transfer resistance, which reveals the activity of methanol electrooxidation. Fig. 5 shows the impedance patterns (A) and phase shift plots (B) of methanol electrooxidation on Pt/MCNTs with various specific surface areas of MCNTs in a solution of 0.5 mol L^{-1} H_2SO_4 containing 0.5 mol L^{-1} CH_3OH at 650 mV (vs. RHE). As we all know, the width of the semicircle is proportional to the charge-transfer resistance of the catalyst material, the smaller the diameter of the semicircle is, and the better the catalytic activity is. It can be observed that diameter of the semicircle increases with the decreasing of the specific surface areas of MCNTs, indicating that the activity of methanol electrooxidation on Pt/MCNTs decreases with the decreasing of the specific surface areas of MCNTs. It is in accordance with the TEM results of Fig. 3 and CV results of Fig. 4. The similar curves can be obtained in Fig. 5(B), indicating the mechanism of methanol electrooxidation on Pt/MCNTs catalysts is the same. EIS studies provide additional evidence that the activity of methanol electrooxidation on Pt/MCNTs-250 catalysts is the highest.

To investigate the stability of catalysts, the accelerated potential cycling test (APCT) within the potential range of 0.6–1.2 V (vs. RHE) was applied. APCT of Pt/MCNTs-250, Pt/MCNTs-120, Pt/MCNTs-60 and Pt/h-MWCNTs-30 are carried out in 0.5 mol L^{-1} H_2SO_4 at 25 °C. Cyclic voltammograms (CV) before and after APCT are shown in Fig. 6. The electrochemical active specific surface area (ESA) is determined through the charge due to hydrogen adsorption/desorption according to the Equation (1). The ESA of different Pt/MCNTs catalysts with cycle number during the APCT are shown in Fig. 7. We will get "relative ESA" by means of the electrochemical active specific surface area (ESA) normalization. The relative ESA of different Pt/MCNTs catalysts with cycle number

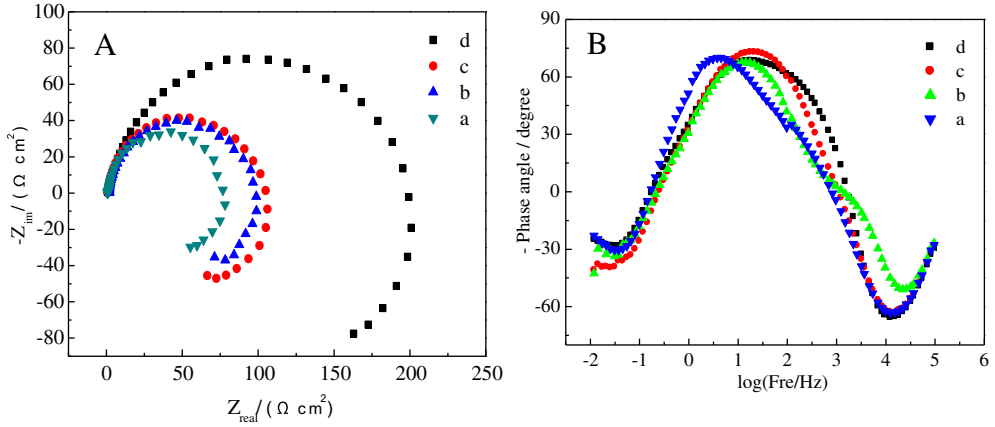

Fig. 5. Impedance patterns (A) and phase shift plots (B) of methanol electrooxidation in 0.5 mol L^{-1} CH_3OH and 0.5 mol L^{-1} H_2SO_4 on Pt/MCNTs with various specific surface areas of MCNTs: (a) 250 m^2 g^{-1}, (b) 120 m^2 g^{-1}, (c) 60 m^2 g^{-1}, and (d) h-MWCNTs with specific surface area 30 m^2 g^{-1}. Polarization potential: 650 mV; test temperature: 25 °C.

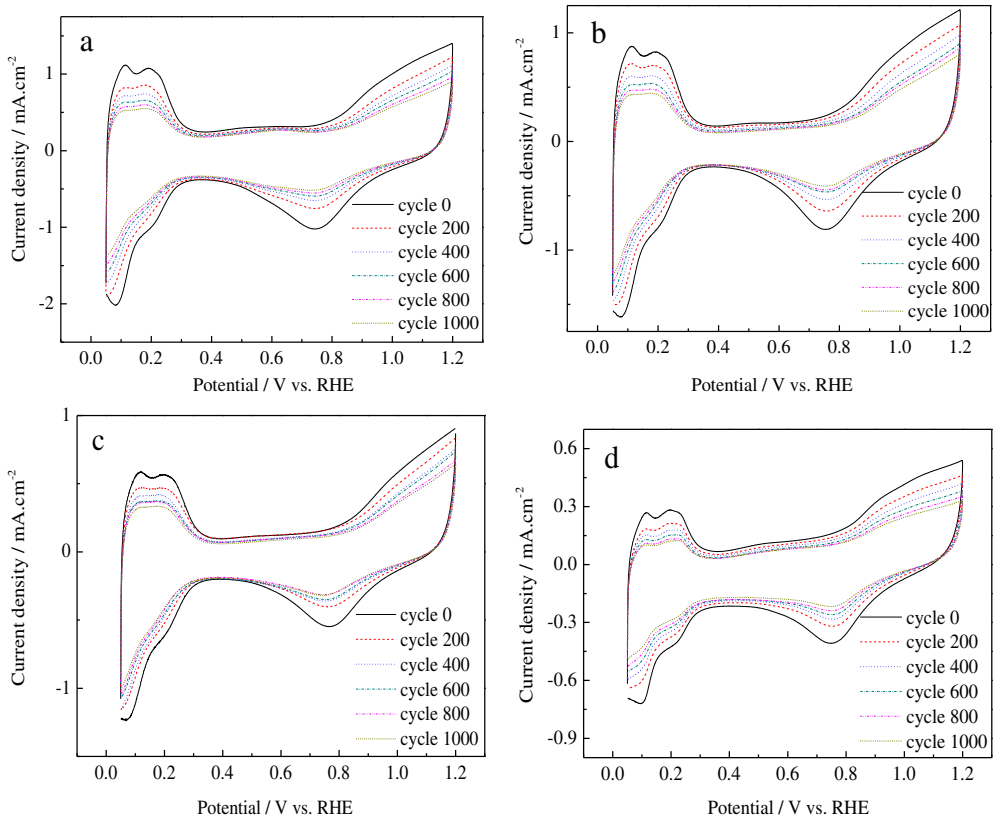

Fig. 6. Cyclic voltammograms in 0.5 mol L^{-1} H_2SO_4 for Pt/MCNTs with various specific surface areas of MCNTs: (a) 250 m^2 g^{-1}, (b) 120 m^2 g^{-1}, (c) 60 m^2 g^{-1}, and (d) h-MWCNTs with specific surface area 30 m^2 g^{-1} during the APCT. Scanning rate: 50 mV s^{-1}; test temperature: 25 °C.

during the APCT are shown in Fig. 8. According to Fig. 7, the original ESA of the catalysts decrease with the decreasing of the specific surface areas of MCNTs which is in accordance with the TEM results of Fig. 3. As we can see, the Pt/MCNTs-250 catalysts show the best initial electrochemical activity. The high performance of Pt/MCNTs-250 can be ascribed to high specific surface areas of CNTs, and well-dispersion in the Pt nanoparticles. However it can be seen that the activity of the Pt/MCNTs-250 is almost the same with that of the Pt/MCNTs-120 and the stability of the Pt/MCNTs-60 catalyst is the best after 1000 cycles APCT. It can be found that the stability of the Pt/MCNTs catalysts is much better than Pt/C. For Pt supported on Vulcan XC-72 carbon, the electrochemical surface area decreases about 70% after the APCT [28]. Shao et al. [21] and Zaragoza-Martín et al. [29] both tested the catalysts at a fixed potential of 1.2 V in 0.5 mol L^{-1} H_2SO_4 during long period time, in which the measurement method of the stability is different from with this work. They got a similar result with us. The degradation rate of Pt/C is about 1.9 times that of Pt/CNTs [21]. The nice corrosion resistance of CNTs might be a key factor. Taking into account the activity and the stability of various Pt/MCNTs catalysts, the optimized specific surface area of MCNTs in the Pt/MCNTs catalysts is 120 m^2 g^{-1}.

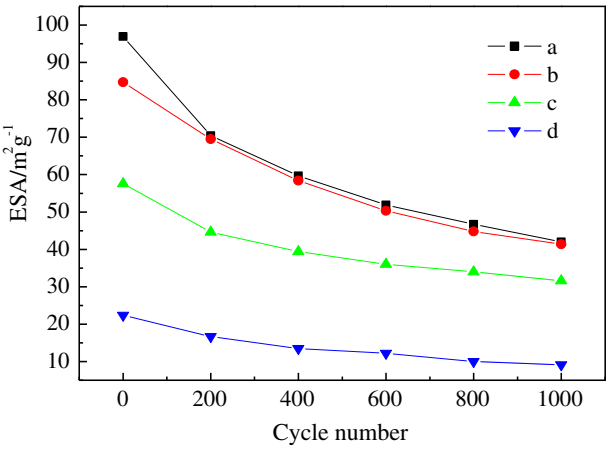

Fig. 7. ESA of Pt/MCNTs with various specific surface areas of MCNTs: (a) 250 m^2 g^{-1}, (b) 120 m^2 g^{-1}, (c) 60 m^2 g^{-1}, and (d) h-MWCNTs with specific surface area 30 m^2 g^{-1}.

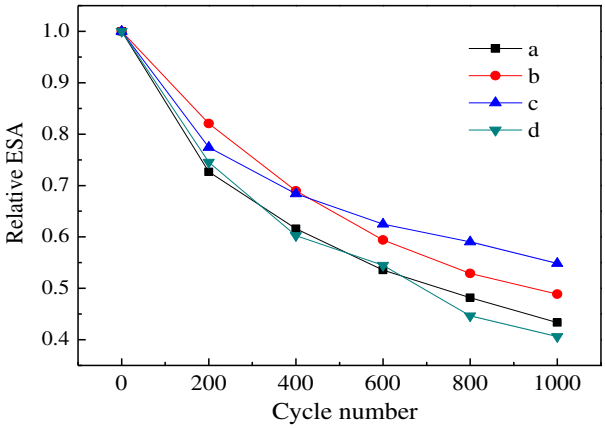

Fig. 8. Relationship of ESA and cycle numbers of Pt/MCNTs with various specific surface areas of MCNTs: (a) 250 m^2 g^{-1}, (b) 120 m^2 g^{-1}, (c) 60 m^2 g^{-1}, and (d) h-MWCNTs with specific surface area 30 m^2 g^{-1}.

4. Conclusions

Pt/MCNTs catalysts have been synthesized by the microwave-assisted polyol process (MAPP). Effect of MCNTs with different specific surface areas on the stability of supported Pt catalysts has been investigated. The experimental results indicate that the original electrochemically active specific surface areas (ESA) and the activity for methanol electrooxidation of the catalysts decrease with the decreasing of the specific surface areas of MCNTs. The results can be ascribed to the high specific surface areas of MCNTs, and well-dispersion in the Pt nanoparticles. Considering the factors of the activity and stability comprehensively, the optimized specific surface area of MCNTs in the Pt/MCNTs catalysts is 120 $m^2\ g^{-1}$. In view of the high electrical conductivity and corrosion resistance of MCNTs, it will highlight the potential utility of MCNTs as catalyst supports in PEMFC applications.

Acknowledgment

We acknowledge the National Natural Science Foundation of China (Grant No. 21273058), China Postdoctoral Science Foundation (Grant No. 2012M520731), Heilongjiang Postdoctoral Financial Assistance (LBH-Z12089) for their financial support.

References

[1] Z.B. Wang, C.R. Zhao, P.F. Shi, Y.S. Yang, Z.B. Yu, W.K. Wang, G.P. Yin, J. Phys. Chem. C 114 (2010) 672–677.
[2] G.J.K. Acres, J. Power Sources 100 (2001) 60–66.
[3] H. Zhang, P.K. Shen, Chem. Rev. 112 (2012) 2780–2832.
[4] Y. Wang, K.S. Chen, J. Mishlera, S.C. Cho, X.C. Adrohera, Appl. Energy 88 (2011) 981–1007.
[5] C. Koenigsmanna, S.S. Wong, Energy Environ. Sci. 4 (2011) 1161–1176.
[6] R. Devanathan, Energy Environ. Sci. 1 (2008) 101–119.
[7] M.K. Debe, Nature 486 (2012) 43–51.
[8] Z.-Z. Jiang, D.-M. Gu, Z.-B. Wang, W.-L. Qu, G.-P. Yin, K.-J. Qian, J. Power Sources 196 (2011) 8207–8215.
[9] Y.Y. Chu, Z.B. Wang, D.M. Gu, G.P. Yin, J. Power Sources 195 (2010) 1799–1804.
[10] B. Fang, N.K. Chaudhari, M.S. Kim, J.H. Kim, J.S. Yu, J. Am. Chem. Soc. 131 (2009) 15330–15338.
[11] E. Antolini, Appl. Catal. B 88 (2009) 1–24.
[12] W. Zhang, J. Chen, G.F. Swiegers, Z.F. Ma, G.G. Wallace, Nanoscale 2 (2010) 282–286.
[13] J. Guo, G. Sun, Q. Wang, G. Wang, Z. Zhou, S. Tang, Carbon 44 (2006) 152–157.
[14] S. Chen, J. Bi, Y. Zhao, L. Yang, C. Zhang, Y. Ma, Q. Wu, X. Wang, Z. Hu, Adv. Mater. 24 (2012) 5593–5597.
[15] Z. Hamoudi, A. Brahim, M.A. El Khakani, Electroanalysis 25 (2013) 538–545.
[16] F. Han, X. Wang, J. Lian, Y. Wang, Carbon 50 (2012) 5498–5504.
[17] T. Matsumoto, T. Komatsu, K. Arai, T. Yamazaki, M. Kijima, H. Shimizu, Y. Takasawab, J. Nakamura, Chem. Commun. (2004) 840–841.
[18] Z. Liu, X. Lin, J.Y. Lee, W. Zhang, M. Han, L.M. Gan, Langmuir 18 (2002) 4054–4060.
[19] Y. Mu, H. Liang, J. Hu, L. Jiang, L. Wan, J. Phys. Chem. B 109 (2005) 22212–22216.
[20] T. Matsumoto, T. Komatsu, H. Nakano, K. Arai, Y. Nagashima, E. Yoo, T. Yamazaki, M. Kijima, H. Shimizu, Y. Takasawa, J. Nakamura, Catal. Today 90 (2004) 277–281.
[21] Y. Shao, G. Yin, Y. Gao, P. Shi, J. Electrochem. Soc. 153 (2006) A1093–A1097.
[22] Z.Z. Jiang, Z.B. Wang, Y.Y. Chu, D.M. Gu, G.P. Yin, Energy Environ. Sci. 4 (2011) 728–735.
[23] Y. Xing, J. Phys. Chem. B 108 (2004) 19255–19259.
[24] T. Belin, F. Epron, Mater. Sci. Eng. B 119 (2005) 105–118.
[25] Z.B. Wang, G.P. Yin, P.F. Shi, J. Electrochem. Soc. 152 (2005) A2406–A2412.
[26] Z.L. Liu, L.M. Gan, H. Liang, W.X. Chen, J.Y. Lee, J. Power Sources 139 (2005) 73–78.
[27] Z.-Z. Jiang, Z.-B. Wang, Y.-Y. Chu, D.-M. Gu, G.-P. Yin, Energy Environ. Sci. 4 (2011) 2558–2566.
[28] M.M. Waje, W.-Z. Li, Z.-W. Chen, P. Larsen, Y.-S. Yan, ECS Trans. 11 (2007) 1227–1233.
[29] F. Zaragoza-Martín, D. Sopeña-Escario, E. Morallón, C. Salinas-Martínez de Lecea, J. Power Sources 171 (2007) 302–309.